ACS APPLIED MATERIALS & INTERFACES

Research Article

www.acsami.org

New Life for an Old Antibiotic

Rahul Kumar Mishra,[†,‡] Elad Segal,[†,‡] Anat Lipovsky,[†] Michal Natan,[∥] Ehud Banin,[∥] and Aharon Gedanken*[,†,§]

[†]Department of Chemistry, Institute of Nanotechnology and Advanced Materials, Bar-Ilan University, Ramat-Gan 52900, Israel

[§]Department of Materials Science and Engineering, National Cheng Kung University, Tainan 70101, Taiwan

[∥]The Mina and Everard Goodman Faculty of Life Sciences, Institute of Nanotechnology and Advanced Materials, Bar-Ilan University, Ramat-Gan 52900, Israel

ABSTRACT: Restoring the antibacterial properties of existing antibiotics is of great concern. Herein, we present, for the first time, the formation and deposition of stable antibiotic nanoparticles (NPs) on graphene oxide (GO) sheets by a facile one-step sonochemical technique. Sonochemically synthesized graphene oxide/tetracycline (GO/TET) composite shows enhanced activity against both sensitive and resistant *Staphylococcus aureus* (*S. aureus*). The size and deposition of tetracycline (TET) nanoparticles on GO can be controlled by varying the sonication time. The synthesized NPs ranged from 21 to 180 nm. Moreover, ultrasonic irradiation does not cause any structural and chemical changes to the TET molecule as confirmed by Fourier transform infrared spectroscopy (FTIR). The virtue of $\pi-\pi$ stacking between GO and TET additionally facilitate the coating of TET NPs upon GO. A time dependent release kinetics of TET NPs from the GO surface is also monitored providing important insights regarding the mechanism of antibacterial activity of GO/TET composites. Our results show that the GO/TET composite is bactericidal in nature, resulting in similar values of minimal inhibitory concentration (MIC) and minimal bactericidal concentration (MBC). This composite is found to be active against TET resistant *S. aureus* at a concentration four times lower than the pristine TET. The sensitive *S. aureus* follows the same trend showing six times lower MIC values compared to pristine TET. GO shows no activity against both sensitive and resistant *S. aureus* even at a concentration as high as 1 mg/mL but influences the biocidal activity of the GO/TET composite. We propose that the unique structure and composition manifested by GO/TET composites may be further utilized for different formulations of antibiotics with GO. The sonochemical method used in this work can be precisely tailored for the stable deposition of a variety of antibiotics on the GO surface to reduce health risks and increase the spectrum of applications.

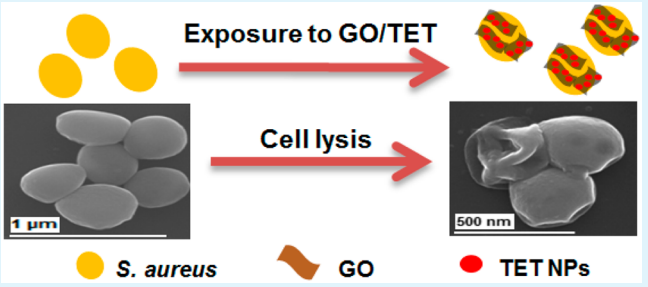

KEYWORDS: *sonochemistry, tetracycline nanoparticles, graphene oxide, antibacterial, bactericidal, S. aureus*

INTRODUCTION

The failure of antibiotic therapy induced by resistant bacteria poses a serious problem on public health worldwide.[1] Life threatening antibiotic resistant species of bacteria have emerged over the past few decades due to extensive misuse of antibiotics. The list of resistant species of bacteria includes multidrug resistant (MDR) and even extremely drug resistant (XDR) strains.[2] These strains of bacteria have evolved to exhibit resistance to almost all the commercially available antibiotics which affects millions of people around the globe.[3] In the ongoing race between the development of new antimicrobial agents and the evolution of antibiotic resistant bacteria, the latter is a winner. Recently many replacements of antibiotics are reported including inorganic nanoparticles,[4−11] quaternary ammonium based compounds,[12] antimicrobial peptides,[13−15] photothermal/photodynamic agents,[16,17] and polymeric cations,[18−23] which can fight the resistant bacteria. In addition to these compounds, many nanoparticle carriers have also been used to encapsulate different antibiotics which show enhanced antimicrobial efficacy. In particular, antibiotics loaded in bovine serum albumin (BSA)[24] and in liposomes,[25] cyanoacrylate nanoparticles (NPs),[26,27] calcium sulfate nanocomposites,[28] and supramolecular gelatin nanoparticles (SGNPs)[29] have been reported. As the pipeline for the development of new antibiotics remains empty, there is an urgent need to explore novel routes to circumvent antibacterial resistance. Therefore, conjugation of existing antibiotics with different substrates (such as graphene oxide (GO)) may provide an alternative solution and give new life to an old antibiotic.

Apart from many applications of graphene in the field of nanoelectronic devices, transparent conductors, and nanocomposite materials,[30−35] it is drawing significant attention for biomedical applications. In recent years, GO has emerged as a versatile nanocarrier to load and control the delivery of a variety

Received: January 19, 2015
Accepted: March 13, 2015
Published: March 13, 2015

DOI: 10.1021/acsami.5b00563
ACS Appl. Mater. Interfaces 2015, 7, 7324−7333

of anticancer drugs. For example, a PEGylated (PEG = polyethylene glycol) nanorange graphene oxide (NGO) has been utilized as a nanocarrier for efficient loading of anticancer drugs via noncovalent physisorption and their cellular uptake behavior has been studied in detail.[36,37] Another anticancer drug, doxorubicin hydrochloride (DOX), has also been successfully loaded on GO, and the release of DOX from GO sheets was explored.[38] Noncovalent strategies appears to be more attractive than covalent ones as the structure of graphene is not tempered in the former and poorly water-soluble drugs can also be loaded on it.[39] Furthermore, efficient loading and targeted delivery of a mixture of anticancer drugs on NGO have been achieved by Zhang and colleagues.[40] These findings indicated that a variety of aromatic drugs can be loaded on GO and their release can be controlled.

Although there are few reports on the synthesis of tetracycline (TET) NPs,[41,42] to the best of our knowledge, in spite of the known interaction between GO and TET through $\pi-\pi$ stacking,[43−45] there has been no efforts to load nanoparticles of any antibiotic on GO. To fill the void for loading and controlled release of nanoantibiotics (NAs) from the GO sheets for antimicrobial applications, we herein present for the first time a sonochemical synthesis of antibiotic nanoparticles (NAs) followed by their successful deposition on GO sheets.

Recently, a simple and cost-effective sonochemical method has been utilized to obtain nanoparticles from inorganic water-soluble salts.[46] Earlier, we have synthesized antimicrobial nanoparticles of metal oxides and metal fluorides.[47−50] These nonwater-soluble nanoparticles demonstrated enhanced antibacterial efficacy as compared to their ionic forms and were successfully deposited on a variety of substrates. The sonochemical process takes advantage of the high-energy collapse of the cavitation bubbles which provides the chemical activation energy required for the synthesis and stabilization of the nanoparticles.[51] This methodology has been utilized for the synthesis of various inorganic materials. Nanoparticles of water-soluble pepsin and amylase have also been successfully coated on various substrates using the sonochemical method and were shown to enhance the catalytic activity compared to their pristine forms.[52,53]

In this manuscript, a sonochemical method is used to synthesize graphene oxide embedded with TET NPs. A homogenous distribution of TET NPs of the smallest particle size of 21 nm on the GO sheets is achieved. The size can be varied as a function of ultrasonication time. In the synthesis process, aqueous solutions of graphene oxide and tetracycline antibiotic were exposed to ultrasonic waves. Fourier transform infrared spectroscopy (FTIR) spectra depicted no change in the chemical structure of TET upon a 5 min ultrasonic irradiation. The successful incorporation of TET NPs on the GO sheets can be attributed to the capability of the high intensity ultrasound to "throw" the NPs onto a surface.[54,55] $\pi-\pi$ interaction due to the presence of the aromatic ring on tetracycline and GO sheets are responsible for the strong adherence of the TET NP on the GO surface. Moreover, the TET/GO composite showed an enhanced antibacterial efficacy against both tetracycline susceptible and resistant *S. aureus* compared to the same concentration of the pristine aqueous solution of tetracycline. The release of TET NPs as a function of time from the GO surface is also monitored and reported. Graphene oxide acts as a stabilizing agent for the TET NPs by facilitating its very high surface area. Thus, the sonochemical method enables one to restore the antibacterial activity of the commercially available tetracycline antibiotic and may present a new methodology to deposit organic nanoparticles on the GO surface to treat susceptible and resistant bacteria. The ability of the sonochemical method to deposit nanoparticles of tetracycline may be further extended to other organic compounds that can be deposited on various surfaces from their solution.

This paper also investigates morphological changes in the bacteria when exposed to different formulations and concentrations of GO, TET, and GO/TET composite. The related mechanism for enhanced efficacy of GO/TET composite compared to the same concentration of pristine TET against *S. aureus* has also been proposed.

EXPERIMENTAL SECTION

Materials. Analytical grade chemicals and deionized water (DDW) were used in all the experiments. Graphite flakes and tetracycline antibiotic (powder) were purchased from Sigma-Aldrich. Hydrogen peroxide (H_2O_2, 30%) and potassium permanganate ($KMnO_4$) were bought from Bio Lab Ltd. (Israel); hydrochloric acid (HCl = 36.46) and sulfuric acid (H_2SO_4 > 98%) were purchased from DAEJUNG Chemicals & Metals Co. Ltd., Korea. Tetracycline (TET) ($C_{22}H_{24}N_2O_8$, HPLC grade) antibiotic was purchased from Sigma-Aldrich. *Staphylococcus aureus* (*S. aureus*) 47302/29 (having intermediate sensitivity to tetraycline) and *S. aureus* B5467161, which is tetracycline sensitive, were collected from clinical specimens in Asaf Ha-Rofe Hospital (Zrifin, Israel). Nutrient broth medium was obtained from BD (Becton, Dickinson and Company).

Synthesis of Graphene Oxide (GO) Sheets. The procedure using the modified Hummer's method for the synthesis of GO is used herein.[56] Briefly, the synthetic steps are as follows: 2 g of graphite flakes was stirred in sulfuric acid (35 mL) for 2 h. Then, 6 g of potassium permanganate was slowly added into the solution, while the temperature was kept constant at 15 °C. After the temperature was stable, the solution was heated and kept at ∼40 °C under constant mixing for 30 min. In the next step, 90 mL of DDW was added carefully to the solution, raising the temperature to ∼98 °C (exothermic reaction) while stirring vigorously for 20 min. The color of the solution changed to dark brown. At the final step, 150 mL of DDW was added, followed by addition of 10 mL of H_2O_2 (30%). The solution was then stirred for another 3 h in order to terminate the reaction and to extract the byproducts (metal ions). The obtained mixture was collected and transferred for further purification with multiple cycles of continuous washing with 5% aqueous HCl. To obtain a neutral (pH ∼ 7) and pure graphite oxide, the product was rewashed and centrifuged with DDW. The brown precipitate was finally dried in a vacuum chamber to get dry graphite oxide powder.

The graphite oxide is then redispersed in DDW to obtain a 1 mg/mL solution. The procedure consists of applying ultrasonic irradiation for 30 min with a titanium horn sonicator at an efficiency of 35% (amplitude), under ice bath conditions to get exfoliated and very thin layers of graphene oxide sheets which are evident in Figure 1.

Preparation of GO/TET Composites. A beaker with 60 mL of graphene oxide aqueous solution (1 mg/mL) was irradiated by a titanium horn sonicator inserted 1 cm into the solution with an efficiency of 35% (amplitude), while keeping the solution under an ice bath and maintaining the temperature at 16 °C for 30 min. Then, the 1 mg/mL (20 mL) aqueous solution of tetracycline (TET) that was prepared ahead was added slowly into the reaction vessel for further sonication at various time intervals (5−20 min). At the end of sonication, the dispersed solution was centrifuged to separate the precipitate.

Determination of TET Concentration in GO/TET Composites. Two methods were utilized to determine the concentration of TET in the GO/TET composites: (a) UV−vis spectroscopy. In order to find the amount of TET NPs coated on GO, we used a simple calibration method with four known concentrations of aqueous TET solutions:

DOI: 10.1021/acsami.5b00563
ACS Appl. Mater. Interfaces 2015, 7, 7324−7333

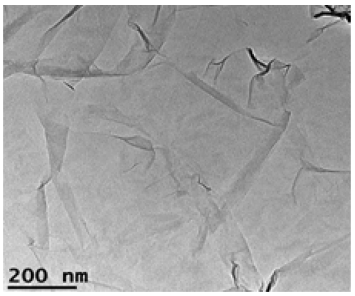

Figure 1. TEM image of very thin transparent sheets of GO after ultrasonication for 30 min in an aq. solution.

0.02 mg/mL (as our 100% mother solution) and three more diluted solutions of TET by adding 2, 1.5, and 1 mL of water into it. After obtaining the absorbance spectra of all the calibration solutions by UV−vis, we extracted the extinction/absorbance coefficient (ε) of the characteristic 365 nm peak of TET by employing the Lambert−Beer's law: $A = \varepsilon Cl$, where A is the absorbance, ε is the extinction/absorbance coefficient [L/mol·cm], C is the concentration [Molar], and l is the thickness of the cuvette (path of light) which is 1 cm.

The ε_0 of TET was found to be 13.1×10^3 [L/mol·cm] at 365 nm; then, we evaluated our genuine samples containing GO/TET, and the solutions were analyzed by UV−vis taking the 365 nm absorbance peak of TET. Our intention was not only to deposit TET in the form of NPs on the GO sheets but also to synthesize smaller size NPs by minimizing the sonication time. All the spectra were normalized for background subtraction to ensure precise calculation. It is important to mention that there is no overlap of the absorption peaks of GO and the TET spectrum, as is expected, since the TET's 365 nm peak is far from the GO absorption peaks (230 and 300 nm). In the second method (b), the supernatant was used throughout this work for all the analysis except H, C, N, and S analysis that probed the precipitate. Prior to this analysis, the precipitate was dried overnight under vacuum and samples were analyzed for H, C, N, and S in the powder form.

In the hydrogen, carbon, nitrogen, and sulfur (H, C, N, S) analysis, three samples of GO/TET precipitate were analyzed for their content of H, C, N, and S. Since, the TET antibiotic is the only source of nitrogens in the GO/TET composite, the amount of TET can be calculated from the HCNS analysis. The value obtained matched well with the UV−vis results, namely, 0.24 mg/mL of TET (both NPs and molecules taken together) deposited on the GO sheets.

Leaching of TET NPs from the GO Sheets. A homogeneous aq. solution of GO/TET of concentration 0.24 mg/mL is equal to the amount of TET deposited on the GO in the form of molecules and NPs. This aq. solution was used as the initial solution for further leaching studies. Six dialysis bags with a pore size of 1000 kDa ("Sartorius lab technology products", Israel) were each filled with 3 mL of the initial solution. Each bag was placed in a beaker containing 50 mL of saline solution with continuous stirring. The leaching samples were taken for analysis from the exterior medium of the corresponding dialysis bags which corresponds to the following: (1) control, 0 h, pure saline, (2) GO + TET, 1 h leaching, (3) GO + TET, 2 h leaching, (4) GO + TET, 6 h leaching, and (5) GO + TET, 24 h leaching. Apart from the above experiment, another control experiment was done, in which 19.2 mg of TET in 80 mL of DDW (0.24 mg/mL) was dissolved without any GO. The resulting solution was filled inside the dialysis bags each containing 3 mL of TET solution. The further experimental procedure was the same as that above-mentioned, to clarify the mechanism of anchoring to GO sheets.

Bacterial Culture. The antibacterial activity of the prepared composite was tested on two bacterial strains: *Staphylococcus aureus* (*S. aureus*) 47302/29 (having intermediate sensitivity to tetraycline) and *S. aureus* B5467161, which is tetracycline sensitive. All bacteria were collected clinical speciemens in Asaf Ha-Rofe Hospital (Zrifin, Israel).

Antibacterial Activity Tests. Antibiotic activity was measured by determination of the MIC (minimal inhibitory concentration). Cultures of bacteria were grown aerobically overnight at 37 °C on plates containing Brain Heart Infusion agar. Colonies were transferred into nutrient broth to obtain an optical density of $A_{660} = 0.1$. Cultures were agitated at 180 rpm to obtain exponential growth ($A_{660} = 0.4$). Concentrations of GO and TET in the experimental solutions were determined to be 1 and 0.24 mg/mL, respectively (as described previously). Stock solution of controls (GO or TET) were prepared to match the above concentrations. Samples of 0.1 mL were spread on plates containing nutrient agar. The minimal bactericidal concentration (MBC) was considered to be the lowest concentration that kills 99.9% of the bacteria. Stock solutions were: (1) pristine tetracycline, 0.24 mg/mL, (2) pristine GO, 1 mg/mL, and (3) GO/TET composite, 0.24 mg TET upon 1 mg GO in 1 mL. Serial dilutions of the GO/TET and GO coated with TET were made in test tubes containing 3 mL of nutrient broth (NB) medium. Fifteen μL of bacterial suspension ($\sim 2 \times 10^8$) was added to the test tubes and incubated with agitation (180 rpm) at 37 °C overnight. The lowest concentration of GO/TET and GO coated with TET, which completely inhibited the visual growth of bacteria (i.e., no turbidity), was recorded as the minimal inhibitory concentration (MIC).

Cell Culture and Cytotoxicity Assay. HeLa cells were cultured in Dulbecco's modified Eagle medium (DMEM, Gibco) supplemented with 10% fetal calf serum (FCS). Where indicated, modified Casamino Acids-DMEM (cDMEM) (0.25 μM $Fe(NO_3)_3$, 1.4 mM $CaCl_2$, 5.4 mM KCl, 0.8 mM $MgSO_4$, 110 mM NaCl, 1 mM Na_2HPO_4, 44 mM $NaHCO_3$, 0.45% glucose, 0.1 M HEPES, 0.1% Casamino Acids) were used instead of DMEM. HeLa cells were seeded at 104 cells/well in a 96-well plate (Greiner Bio-One) and incubated at 37 °C in a humidified atmosphere of 5% CO_2. On the following day, HeLa cells were washed twice with cDMEM and then supplemented with one of the following solutions: pristine TET (7 μg/mL), GO (7 μg/mL), GO + TET compound (7 μg/mL), DDW, and cDMEM (control). Following an overnight incubation at 37 °C in which the cells were exposed to the aforementioned solutions, the cytotoxicity assay was conducted using Promega's CytoTox-ONE homogeneous membrane integrity assay according to the manufacturer's instructions.

Scanning Electron Microscopy Preparation Protocol. The fixation of samples was performed by the triple fixation of the GTGO (glutaraldehyde−tannic acid−guanidine hydrochloride−osmium tetraoxide) method for ESEM.[57] Briefly, the samples were fixed with 2.5%/2% glutaraldehyde/paraformaldehyde in phosphate buffer (pH 7.2), followed by postfixation in 2% tannic acid−guanidine hydrochloride. The third fixative was done with 2% OsO_4. After fixation, the cells were dehydrated in graded ethanol solutions; then, the ethanol was exchanged by Freon 113-tf again using graded solutions. Finally, the samples were air-dried and carbon coated for further analysis by ESEM.

Instrumentation. Ultrasonic irradiation for all the samples was done by a titanium horn sonicator (Sonics & Materials, VCX-750). The absorption spectrum of graphene oxide (UV−visible) was recorded on a CARY bio-100 spectrophotometer. For the X-ray photoelectron spectroscopy (XPS) analysis, the Kratos Axis HS spectrometer with an Al Kα X-ray radiation source (photon energy 1486.6 eV) was used. The imaging, morphology, and topography of graphene oxide sheets and graphene oxide/TET composites were studied by the transmission electron microscope (TEM) JEOL jem-1400 (120 kV). GO, TET, and GO/TET with *S. aureus* were also studied by an environmental scanning electron microscope (ESEM) employing the FEI QUANTA 200F device. The FTIR spectra were recorded using an Avarter model FT-IR spectrometer in the range of 4000−1000 cm^{-1}.

The total nitrogen, carbon, sulfur, and hydrogen of selected materials were analyzed using the CHNS analyzer model FLASH EA 1112 series made by Thermo Finnigan, Italy. During analysis, combustion of a sample occurs at 1000 °C to produce gases of H_2O, CO_2, and N_2. The mixture of the gases was separated by a gas chromatography (GC) column.

DOI: 10.1021/acsami.5b00563
ACS Appl. Mater. Interfaces 2015, 7, 7324−7333

RESULTS AND DISCUSSION

A facile and environmentally friendly method was developed to synthesize the GO/TET composite using ultrasound as a tool to deposit TET NPs on the GO sheets. GO sheets contain many oxygenated reactive functional groups, like carboxylic groups as the edge group and phenol hydroxyl and epoxy functional groups on its basal plane with the presence of many aromatic regions as part of the GO surface.[58,59] These exposed aromatic regions act as an anchoring site which facilitated the adsorption of tetracycline nanoparticles on its surface. Moreover, sonochemistry also helps to facilitate the interaction of GO and TET. This method provides both physical energy and a path due to the high energy released upon the collapse of the acoustic bubbles, creating microjets after this phenomenon. These microjets moving at high speeds (>500 m/s) throw the newly formed TET NPs onto the GO sheets, which were found to be appropriate substrates for the antibiotic NPs.[51] Graphene oxide (GO) is chosen as a substrate for its fascinating properties to adsorb aromatic organic compounds on its surface.[60,61] This ability of GO is harnessed to deposit antibiotic NPs on GO sheets via $\pi-\pi$ interactions, and the TET NPs are adhered to the GO because of this interaction.

Direct evidence for the formation of very thin and almost transparent GO sheets is depicted by transmission electron microscopy (TEM). Figure 1 shows ultrasonically exfoliated GO sheets for 30 min in an aq. solution.

To further confirm the formation of GO, the UV−vis spectrum was recorded. The UV−vis absorption measurement shows the characteristic peaks of graphene oxide at 233 nm assigned to $\pi-\pi^*$ transitions of the aromatic C═C bonds. The shoulder at 303 nm was attributed to $n-\pi^*$ transitions of the C═O bonding (Figure 2).

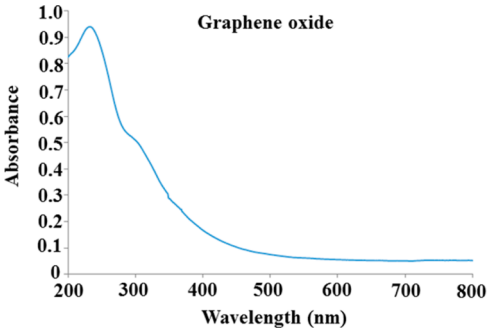

Figure 2. UV−vis spectrum of graphene oxide showing the characteristic peaks of the C═C and C═O functional groups.

To examine the state of the chemical composition of GO prepared by the modified Hummer's method, X-ray photoelectron spectroscopy (XPS) was used. Figure 3 shows the XPS C 1s spectra of GO which is an overlap of four peaks 284.9, 285.9, 287.1, and 289.2 eV, showing the fingerprints of C−C, C−O, C═O, and C(═O)-(OH) bonds, respectively.[62]

Ultrasonic Deposition of TET NPs on the GO Sheets. Prior to depositing NPs of TET on the GO sheets, we tried to form the NPs of TET in water by ultrasound irradiation. TEM measurements of a drop of the sonicated solution did not reveal the formation of stable NPs. The pristine TET molecules show agglomeration of molecules (Figure 4a) resulting in amorphous structures, while 5 min of ultrasound irradiation leads to defined spherical structures aggregated to a micrometer size (Figure 4b).

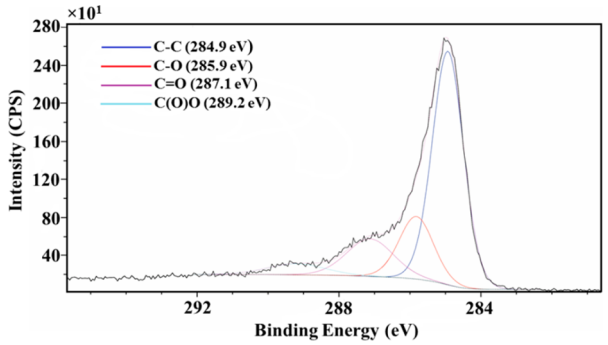

Figure 3. X-ray photoelectron spectroscopy (XPS) of GO showing C 1s spectra.

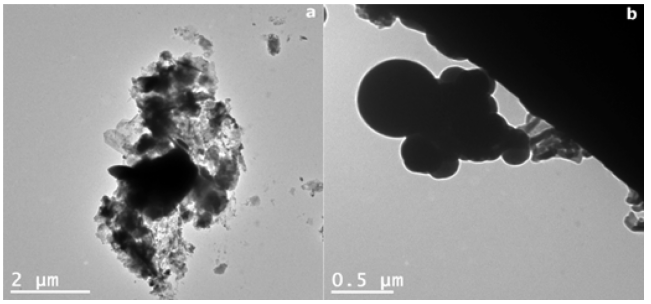

Figure 4. Transmission electron microscopy images of (a) pristine TET and (b) 5 min ultrasonicated TET.

Sonochemical coating of TET NPs on the GO surface is intended to prevent the formation of TET aggregates as illustrated in Scheme 1. The solutions containing GO and TET were exposed to ultrasonic irradiation for 5, 10, and 20 min under ice bath conditions. The deposition of TET NPs on the GO sheets was observed for all these sonication times. The size of TET nanoparticles and their coated amount depends on the sonication time. As the time increased from 5 to 10 to 20 min, the size of the coated TET NPs also increased. For 5 and 10 min ultrasonic irradiation, the average sizes were 21 and 130 nm, respectively. For 20 min ultrasonic irradiation, the average size of TET NPs was 180 nm. Transmission electron microscopy images of the deposited TET NPs on the GO sheets with varying sonication times are shown in Figure 5.

As detailed in the Experimental Section, the absorbance spectrum was measured before and after the deposition, and the concentration of the TET associated with GO was calculated to be 0.24 mg/mL. The conversion and deposition of TET molecules in the form of NPs on the GO sheets was calculated to be 4%. The low conversion percentage is due to the short sonication time (5 min), but it is also the optimal one. The absorbance spectrum of graphene oxide, tetracycline, and GO/TET composite is given in Figure 6, for comparison. The spectra is normalized, and the obtained concentration of TET upon GO is 0.24 mg/mL. The obtained concentration of TET upon GO (0.24 mg/mL) is in congruence with HCNS analysis.

Confirmation of Unchanged Chemical Structure of Pristine TET Compared with TET upon Ultrasonic Irradiation. Since ultrasonic irradiation was employed to form and deposit TET NPs on the GO sheets, we, therefore, evaluated whether this process may affect the chemical composition of the TET molecules. Fourier transform infrared spectroscopy (FTIR) was performed for the characterization of pristine TET as well as for the sample irradiated sonochemically

DOI: 10.1021/acsami.5b00563
ACS Appl. Mater. Interfaces 2015, 7, 7324−7333

Scheme 1. Schematic Depiction of the Sonochemical Preparation of GO/TET Composites

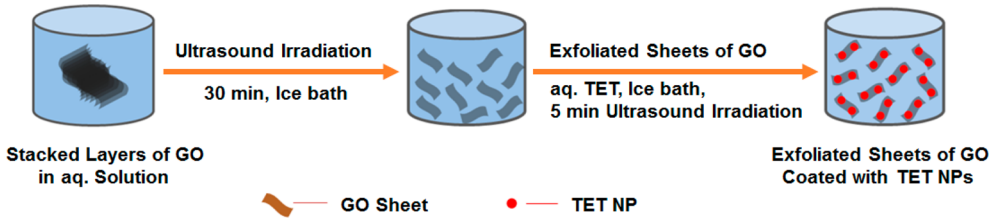

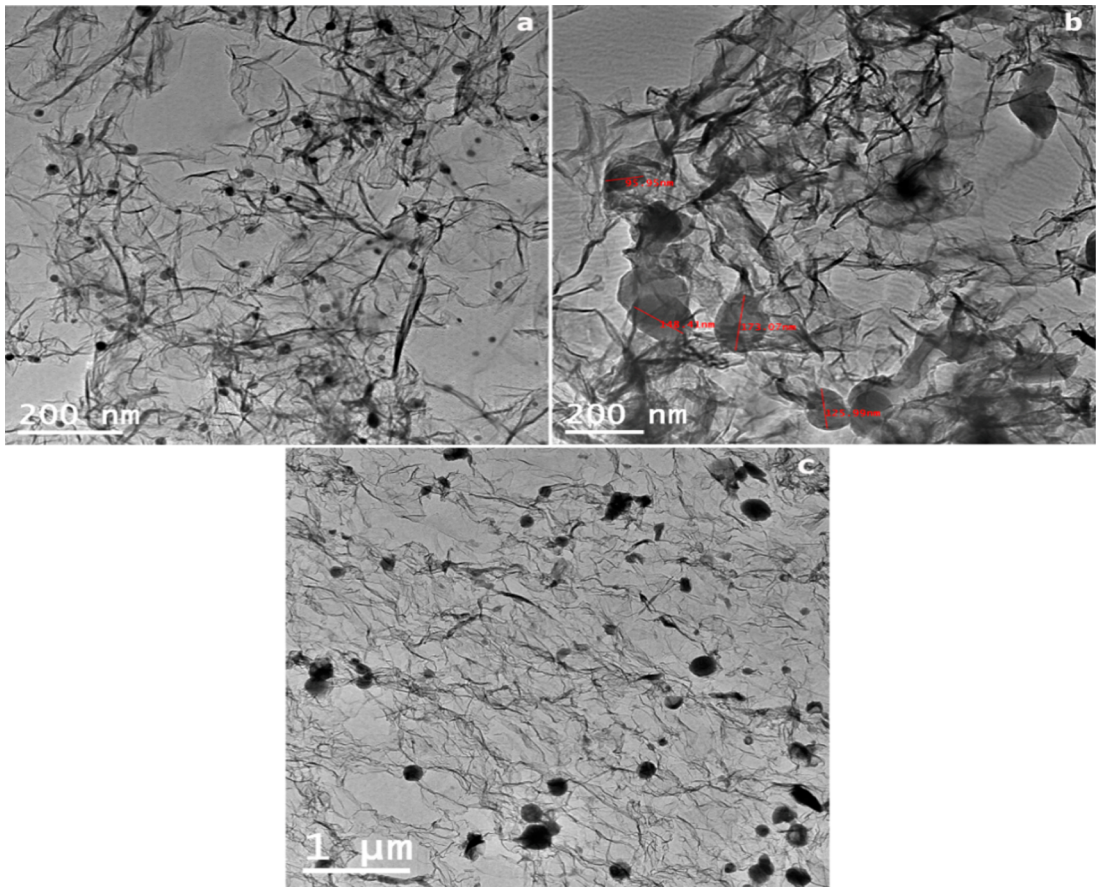

Figure 5. TEM images of TET NPs deposited on GO sheets with the change in size as a function of ultrasonication time of (a) 5 min, (b) 10 min, and (c) 20 min.

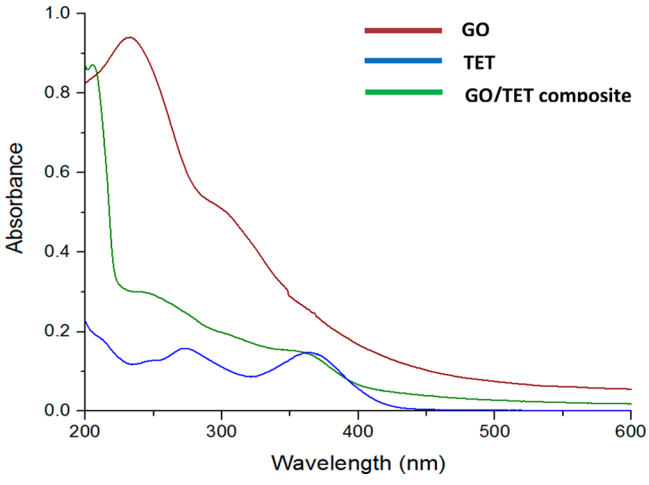

Figure 6. Normalized absorbance spectrum of GO, TET, and GO/TET composite in which a concentration of 0.24 mg/mL is obtained.

for 5 min. The concentration of aq. TET used for the FTIR measurements was 1 mg/mL. In addition, the FTIR spectrum of the 5 min sonicated TET sample was also measured. The representative vibrational peaks for TET are 1463, 1540, 1577, and 3696 cm^{-1}, which was found to be unchanged, and no new absorption peaks were detected. These peaks are assigned to vibrations of C−N, N−H, C═O, and O−H, respectively (Figure 7). Furthermore, no additional peaks were observed. The FTIR characterization shows that the TET molecules do not undergo chemical changes for the 5 min ultrasonic irradiation.

Highly Effective Bactericidal Activity of GO/TET Composites. The antibacterial activities of GO, TET, and GO/TET composites were compared on both TET sensitive and resistant *S. aureus*. The minimal inhibitory concentration (MIC) and minimal bactericidal concentration (MBC) determinations for GO, TET, and GO/TET composite were determined by the broth dilution method in tubes containing nutrient broth and appropriate dilutions of the formulations

DOI: 10.1021/acsami.5b00563
ACS Appl. Mater. Interfaces 2015, 7, 7324−7333

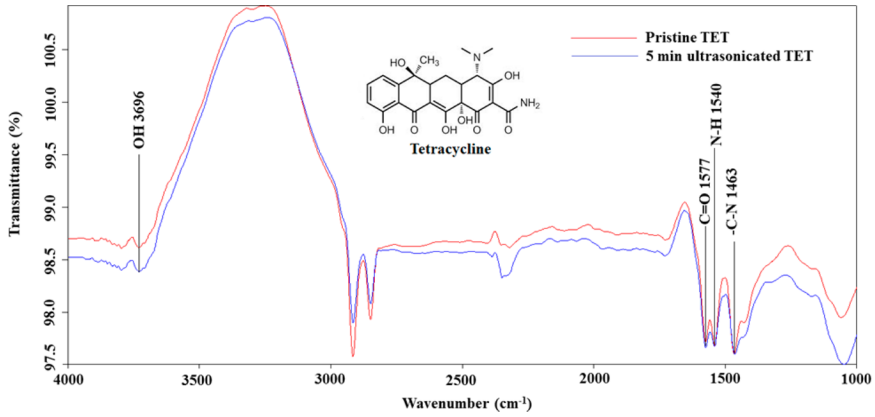

Figure 7. FTIR spectra of a pristine and 5 min ultrasonicated TET aqueous solution. The spectra show no change in the chemical structure of TET upon 5 min ultrasonic irradiation.

tested (made from the stock solution). The MIC was recognized as the lowest concentration that prevented visible growth after 24 h of incubation at 37 °C. To determine the MBC, the MIC tube and all the tubes without visual turbidity were sampled. The minimal inhibitory concentration of GO/TET against the resistant *S. aureus* (02/29) was more than 4 times lower as compared to pristine TET (Figure 8). Similar

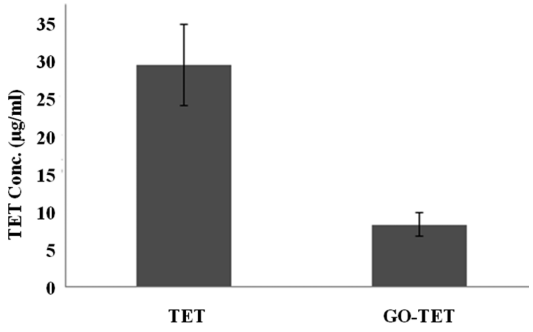

Figure 8. Illustration of MIC values of TET and GO/TET composite for resistant bacteria.

trends were observed with sensitive bacteria (*S. aureus* 161) in which the MIC value was reduced by a factor of 6 (from 0.366 μg/mL of TET to 0.06 μg/mL of GO/TET). GO alone did not affect bacteria even at a concentration as high as 1 mg/mL. Since the MIC and MBC values for GO/TET was the same, it can be claimed that GO/TET reacts on *S. aureus* as a bactericidal agent. The comparison of MIC values between pristine TET and GO/TET composite is shown in Figure 8.

Morphological Changes in Bacteria after Exposure to GO/TET Composites. The GO/TET composites were highly bactericidal for *S. aureus*, but for a better understanding of the biological basis for the bactericidal activity of the GO/TET composites, the effect of different formulations of GO and TET on bacterial morphology was analyzed by electron microscopy. *S. aureus* cells were incubated with a sublethal concentration of all formulations and photographed after fixation and carbon coating.

ESEM analysis revealed clear morphological changes of the treated bacteria cell (Figure 9c,d) compared to the untreated (control) cells (Figure 9a). GO sheets were also visible near or on the bacterial cell (Figure 9b). The GO/TET composite treated cells exhibited a wide variety of cell disfigurations. For example, an increased surface roughness and presence of holes

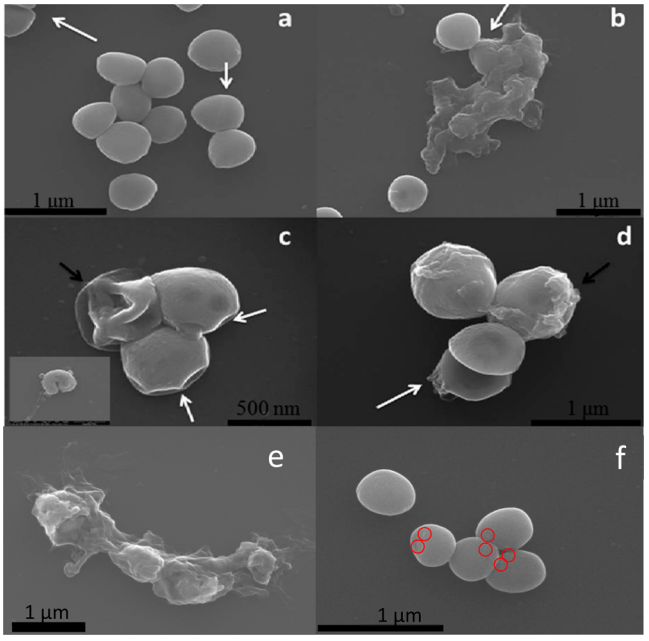

Figure 9. ESEM images of different composites with *S. aureus*: (a) control, only *S. aureus*, (b) only GO, (c, d) GO/TET composites with *S. aureus*, (e) higher magnification of the GO sheets (from GO/TET composite), and (f) perfectly undamaged *S. aureus* exposed to free TET.

(pits) in the cellular membrane were observed, (Figure 9c, white arrow) which implies a cell wall perforation. In other cases, complete deformation of the cellular structure is visible (Figure 9c, black arrow and inset). Cell lysis (burst) was also shown (Figure 9d, white arrow). The pristine GO sheets and the GO/TET composites were found to be attached to the cell surfaces. Two modes of contact were observed: (1) cell-wrapping, the GO/TET composites completely covered the cellular membrane practically engulfing the cell, and (2) the cells were attached to the GO surface (Figure 9b). In contrast to the treated cells, the control cells are perfectly round with a smooth membrane; some of the cells are dividing with visible septa (Figure 9a, marked by white arrows). A higher magnification of the GO sheets is visible in Figure 9e. In addition, the unharmed bacteria cells, which are exposed to free TET (Figure 9f), give strong evidence for our bactericidal activity results. The red circles indicate TET particles which are

DOI: 10.1021/acsami.5b00563
ACS Appl. Mater. Interfaces 2015, 7, 7324−7333

in contact with the bacteria cell membranes but cause no visible damage.

One of the main questions is the increased activity of the GO/TET composites in comparison to pristine TET. In fact, the unique structure of the GO/TET composites overcomes one of the bacterial resistance mechanisms. Bacteria usually acquire resistance to tetracycline from horizontal transfer of a gene that encodes an efflux pump. Efflux pumps actively eject tetracycline from the cell, preventing the buildup of an inhibitory concentration of tetracycline in the cytoplasm.[63] The concentrated presence of antibiotic which is coated upon GO sheets, most probably, overcomes the active ejection, allowing toxic buildup of TET concentration. Additionally, an important factor that can affect the antibacterial activity of the GO/TET composites is the GO sheets itself. It is also plausible that the direct contact of the cell surface with graphene oxide causes membrane stress[64] and may facilitate the penetration of the antibiotics.

Release of TET from the GO/TET Composites. The next step was to study and clarify the stability of the GO/TET composites, and the release kinetics of TET NPs to saline was probed by UV−vis spectroscopy. The release of TET NPs from the GO surface was followed at the selected time points ranging from 0 to 24 h (as calculated by UV−vis absorbance values). Understanding the release of the nanoparticles from the surface of GO can give us important insights regarding the affinity of TET NPs to the surface. Another question that can be answered by these studies is the mechanism of bacteria killing. It is well-known that TET antibiotic has to enter the cell in order to kill the bacteria. It is desired that, if the TET NPs should be the killing agents and not the individual molecules, the release of the antibiotic from the composite should be low enough to ensure the activity of the NPs. The percentage of TET that leached out versus time is illustrated in Figure 10.

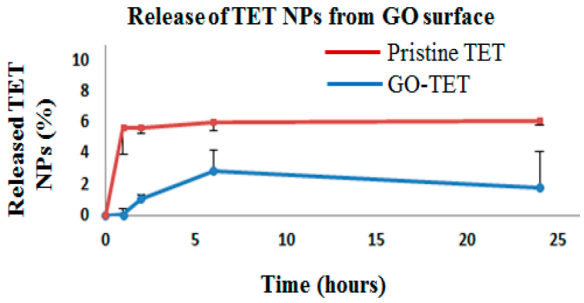

Figure 10. Comparison of pristine TET and GO/TET release profiles into saline as a function of time; the largest amount is leached after 6 h for the GO/TET composite. For GO/TET, the amount leached out after 6 h is only 2.9%. Error bars represent the standard deviation.

The highest amount of leaching is obtained after 6 h, which corresponds to 2.9% of the initial TET concentration on the GO; after this time point, the values slightly decrease due to equilibrium conditions between GO/TET inside the dialysis bag and the saline medium outside the dialysis bag. In addition, a comparison graph of the release profile of pristine TET and GO/TET composite is plotted.

The extremely low leaching of the antibiotic from the GO sheets suggests first that the bacterial killing is done by the solid GO/TET composites and not by the aqueous TET solution. Second, it points to a stable product in which (as seen from the ESEM images) the GO acts as a "death trap" to bacteria by surrounding/attaching[64] to it while releasing TET antibiotic from the surface and killing the bacteria. The release profile of GO/TET composites are also compared with the pristine aq. TET solution under the same conditions. The leaching of pristine aq. TET solution is faster than aq. GO/TET solution. This is due to the absence of GO in the case of aq. pristine TET, which acts as an anchor for most of the aromatic molecules.[60,61]

The fact that only 2.9% of TET was released from the GO surface can teach us about the strong affinity of TET toward GO. This adherence is attributed to two factors; first, to the intrinsic chemical properties of GO and TET, and second, to the sonochemical irradiation that forms the TET NPs and then leads to fast moving microjets that are created following the collapse of the acoustic bubble. These microjets are "throwing" the newly formed TET NPs on the GO surface. The continuous release of 2.9% TET from the GO surface, which corresponds to ∼7 μg/mL, is considered to be enough even for inhibition of the resistant *S. aureus*. Table 1 presents the absorbance values as a function of leaching time of the analyzed samples; TET's absorption at the 365 nm peak was used for the calculations for all the leaching experiments.

Table 1. Absorbance Data of the Solution Obtained for Various Leaching Times of TET NPs Removed from the GO Surface

time of leaching (hours)	absorbance (365 nm peak of TET)
0	0
1	0.00323
2	0.07533
6	0.20523
24	0.12447

Taking into account the morphological changes in the bacteria when exposed to different formulations of GO and TET including the GO/TET composite, the antibacterial results of MIC/MBC, and the leaching studies, the proposed mechanism is as follows: the bacterial surface is attached to the GO sheets and TET antibiotic is released from GO surface (by natural leaching and probably due to mechanical "scratching" by the bacteria adhered on the GO surface). When the antibiotic is released in the proximity of the bacteria, a toxic concentration is built up, killing the cells. The killing of the resistant bacteria is due to the amount of the antibiotic entering the cell; i.e., one NP of TET contains at least 10,000 molecules, overcoming the rate by which the TET molecules are rejected from the bacterial cell by the efflux pumps.[63]

Cytotoxicity Assays of Graphene Oxide, Tetracycline, and the GO/TET Composite. The potential use of combining TET NPs with GO for various medical applications raises the need to examine the potential cytotoxicity effect of these agents. To evaluate the potential of GO/TET to exert cytotoxicity, we conducted the CytoTox-ONE membrane integrity assay on the HeLa cell line exposed to one of the following: pristine TET (7 μg/mL), GO (7 μg/mL), GO + TET compound (7 μg/mL), DDW, or cDMEM (control). As shown in Figure 11, none of the reagents applied exerted toxicity as compared with the negative control (i.e., cDMEM). On the contrary, the positive control (i.e., lysis buffer) caused a severe toxicity to the cells, as can be expected.

In this assay, we have taken the highest concentration of GO/TET composite (7 μg/mL) because it corresponds to the

DOI: 10.1021/acsami.5b00563
ACS Appl. Mater. Interfaces 2015, 7, 7324−7333

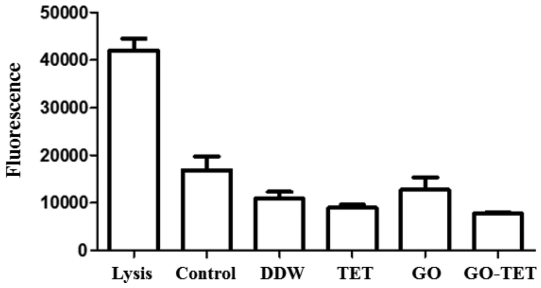

Figure 11. Cytotoxicity results obtained, clearly showing that GO/TET composite is not toxic to HeLa cells. HeLa cells were exposed for 20 h to one of the reagents depicted on the graph. Cytotoxicity was assessed by the CytoTox-ONE homogeneous membrane integrity assay. The values present the average of 4 repeats.

MIC value of the resistant *S. aureus*. As one can observe in Figure 11, even pristine TET and DDW were more cytotoxic compared to GO/TET. It is worth mentioning here that the MIC value of the GO/TET composite on sensitive *S. aureus* is 0.06 μg/mL, which is more than 100 times lower than the MIC value of the resistant *S. aureus* (7 μg/mL). Both (0.06 and 7 μg/mL) concentrations are successful in eliminating the sensitive and resistant *S. aureus*, respectively, but show no evident cytotoxicity to these human cells. Therefore, the designed GO/TET composite offers a safer platform for drug repositioning and has potential to be integrated in pharmaceutical development.

CONCLUSIONS

In this study, a facile, environmentally friendly, one-step, time saving sonochemical method was used to synthesize GO/TET composites. Our GO/TET composites revealed superior antibacterial activity against both TET sensitive and resistant *S. aureus* compared to the same concentration of pristine aqueous TET solution. Superior MIC values of 7 μg/mL for GO/TET composites were observed against resistant *S. aureus*, which was four times lower than the pristine TET MIC values (30 μg/mL). Sensitive *S. aureus* also showed a similar trend for which the MIC value was reduced from 0.366 μg/mL for pristine TET to 0.06 μg/mL for GO/TET, i.e., by a factor of 6. A very high concentration of 1 mg/mL of GO showed no antibacterial effect against both sensitive and resistant *S. aureus*. The GO/TET composite may be claimed to be a bactericidal agent as the MIC and MBC values for different formulations of GO and TET were found to be the same. The unique structure of the GO/TET composite facilitated the intimate contact of bacteria with TET NPs which was found to be responsible for the enhanced antibacterial activity. The acquired resistance of bacteria is commonly associated with an active efflux pump by which antibiotics are thrown out of the bacterial cytoplasm before reaching an effective intrabacterial concentration. The functions of GO/TET composites are synergistic. Our results suggest that the GO engulfs the bacteria from all sides providing an active surface for cell adherence causing membrane stress. It is then assumed that the TET NP enriched GO sheets allow time dependent release of TET NPs causing intrabacterial concentration to reach an effective and lethal value through cell penetration, overcoming the active efflux pump which cannot throw out all the TET molecules thereby causing cell lysis. The cytotoxicity assay performed on HeLa cells does not show any evidence for the GO/TET composite to be toxic. Moreover, the GO/TET composite is even less cytotoxic than commercially available pristine TET and DDW. We believe that many possible applications can be manifested in the field of drug repositioning and pharmaceutical formulations of existing antibiotics with GO can be developed from the findings of the current study. Similar to GO/TET composites, other developments such as surface coating of fabrics, glass, and medical devices as a disinfecting agent can be explored.

AUTHOR INFORMATION

Corresponding Author

*E-mail: Aharon.Gedanken@biu.ac.il.

Author Contributions

‡R.K.M. and E.S. contributed equally.

Notes

The authors declare no competing financial interest.

ACKNOWLEDGMENTS

The authors thank Dr. Ulyana Shimanovich, from the Department of Chemistry, University of Cambridge (UK), for fruitful discussions. A. Gedanken and E. Banin thank the TEVA company for supporting this research.

REFERENCES

(1) Rizzello, L.; Pompa, P. P. Nanosilver-Based Antibacterial Drugs and Devices: Mechanisms, Methodological Drawbacks, and Guidelines. *Chem. Soc. Rev.* **2014**, *43*, 1501−1518.

(2) Andersson, D. I.; Hughes, D. Antibiotic Resistance and Its Cost: Is It Possible to Reverse Resistance? *Nat. Rev. Microbiol.* **2010**, *8*, 260−271.

(3) Blecher, K.; Nasir, A.; Friedman, A. The Growing Role of Nanotechnology in Combating Infectious Disease. *Virulence* **2011**, *2*, 395−401.

(4) Agarwal, A.; Guthrie, K. M.; Czuprynski, C. J.; Schurr, M. J.; McAnulty, J. F.; Murphy, C. J.; Abbott, N. L. Polymeric Multilayers that Contain Silver Nanoparticles Can Be Stamped onto Biological Tissues to Provide Antibacterial Activity. *Adv. Funct. Mater.* **2011**, *21*, 1863−1873.

(5) Lee, J. S.; Murphy, W. L. Functionalizing Calcium Phosphate Biomaterials with Antibacterial Silver Particles. *Adv. Mater.* **2013**, *25*, 1173−1179.

(6) Zhao, Y.; Tian, Y.; Cui, Y.; Liu, W.; Ma, W.; Jiang, X. Small Molecule-Capped Gold Nanoparticles as Potent Antibacterial Agents that Target Gram-Negative Bacteria. *J. Am. Chem. Soc.* **2010**, *132*, 12349−12356.

(7) Lv, M.; Su, S.; He, Y.; Huang, Q.; Hu, W.; Li, D.; Fan, C.; Lee, S. T. Long-Term Antimicrobial Effect of Silicon Nanowires Decorated with Silver Nanoparticles. *Adv. Mater.* **2010**, *22*, 5463−5467.

(8) Zhang, D.; Zhao, Y.-X.; Gao, Y.-J.; Gao, F.-P.; Fan, Y.-S.; Li, X.-J.; Duan, Z.-Y.; Wang, H. Anti-Bacterial and in Vivo Tumor Treatment by Reactive Oxygen Species Generated by Magnetic Nanoparticles. *J. Mater. Chem. B* **2013**, *1*, 5100−5107.

(9) Ocsoy, I.; Paret, M. L.; Ocsoy, M. A.; Kunwar, S.; Chen, T.; You, M.; Tan, W. Nanotechnology in Plant Disease Management: DNA-Directed Silver Nanoparticles on Graphene Oxide as an Antibacterial against *Xanthomonas perforans*. *ACS Nano* **2013**, *7*, 8972−8980.

(10) Qi, G.; Li, L.; Yu, F.; Wang, H. Vancomycin-Modified Mesoporous Silica Nanoparticles for Selective Recognition and Killing of Pathogenic Gram-Positive Bacteria over Macrophage-Like Cells. *ACS Appl. Mater. Interfaces* **2013**, *5*, 10874−10881.

(11) Li, L. L.; Wang, H. Enzyme-Coated Mesoporous Silica Nanoparticles as Efficient Antibacterial Agents in Vivo. *Adv. Healthcare Mater.* **2013**, *2*, 1351−1360.

(12) Buffet-Bataillon, S.; Tattevin, P.; Bonnaure-Mallet, M.; Jolivet-Gougeon, A. Emergence of Resistance to Antibacterial Agents: The

DOI: 10.1021/acsami.5b00563
ACS Appl. Mater. Interfaces 2015, 7, 7324−7333

Role of Quaternary Ammonium Compounds–A Critical Review. *Int. J. Antimicrob. Agents* **2012**, *39*, 381−389.
(13) Some, S.; Ho, S. M.; Dua, P.; Hwang, E.; Shin, Y. H.; Yoo, H.; Kang, J. S.; Lee, D. K.; Lee, H. Dual Functions of Highly Potent Graphene Derivative-Poly-L-Lysine Composites to Inhibit Bacteria and Support Human Cells. *ACS Nano* **2012**, *6*, 7151−7161.
(14) Salick, D. A.; Pochan, D. J.; Schneider, J. P. Design of an Injectable Beta-Hairpin Peptide Hydrogel That Kills Methicillin-Resistant *Staphylococcus aureus*. *Adv. Mater.* **2009**, *21*, 4120−4123.
(15) Liu, L.; Xu, K.; Wang, H.; Tan, P. K.; Fan, W.; Venkatraman, S. S.; Li, L.; Yang, Y. Y. Self-Assembled Cationic Peptide Nanoparticles as an Efficient Antimicrobial Agent. *Nat. Nanotechnol.* **2009**, *4*, 457−463.
(16) Wu, M. C.; Deokar, A. R.; Liao, J. H.; Shih, P. Y.; Ling, Y. C. Graphene-Based Photothermal Agent for Rapid and Effective Killing of Bacteria. *ACS Nano* **2013**, *7*, 1281−1290.
(17) Li, Y.; Zhang, W.; Niu, J.; Chen, Y. Mechanism of Photogenerated Reactive Oxygen Species and Correlation with the Antibacterial Properties of Engineered Metal-Oxide Nanoparticles. *ACS Nano* **2012**, *6*, 5164−5173.
(18) Adhikari, M. D.; Goswami, S.; Panda, B. R.; Chattopadhyay, A.; Ramesh, A. Membrane-Directed High Bactericidal Activity of (Gold Nanoparticle)-Polythiophene Composite for Niche Applications against Pathogenic Bacteria. *Adv. Healthcare Mater.* **2013**, *2*, 599−606.
(19) Lee, H.; Lee, Y.; Statz, A. R.; Rho, J.; Park, T. G.; Messersmith, P. B. Substrate-Independent Layer-by-Layer Assembly by Using Mussel-Adhesive-Inspired Polymers. *Adv. Mater.* **2008**, *20*, 1619−1623.
(20) Li, P.; Zhou, C.; Rayatpisheh, S.; Ye, K.; Poon, Y. F.; Hammond, P. T.; Duan, H.; Chan-Park, M. B. Cationic Peptidopolysaccharides Show Excellent Broad-Spectrum Antimicrobial Activities and High Selectivity. *Adv. Mater.* **2012**, *24*, 4130−4137.
(21) Zhou, Y.; Huang, W.; Liu, J.; Zhu, X.; Yan, D. Self-Assembly of Hyperbranched Polymers and Its Biomedical Applications. *Adv. Mater.* **2010**, *22*, 4567−4590.
(22) Ng, V. W.; Ke, X.; Lee, A. L.; Hedrick, J. L.; Yang, Y. Y. Synergistic Co-Delivery of Membrane-Disrupting Polymers with Commercial Antibiotics against Highly Opportunistic Bacteria. *Adv. Mater.* **2013**, *25*, 6730−6736.
(23) Semiramoth, N.; Di Meo, C.; Zouhiri, F.; Said-Hassane, F.; Valetti, S.; Gorges, R.; Nicolas, V.; Poupaert, J. H.; Chollet-Martin, S.; Desmaele, D.; Gref, R.; Couvreur, P. Self-Assembled Squalenoylated Penicillin Bioconjugates: An Original Approach for the Treatment of Intracellular Infections. *ACS Nano* **2012**, *6*, 3820−3831.
(24) Avivi, S.; Nitzan, Y.; Dror, R.; Gedanken, A. An Easy Sonochemical Route for the Encapsulation of Tetracycline in Bovine Serum Albumin Microspheres. *J. Am. Chem. Soc.* **2003**, *125*, 15712−15713.
(25) Drulis-Kawa, Z.; Dorotkiewicz-Jach, A. Liposomes as Delivery Systems for Antibiotics. *Int. J. Pharm.* **2010**, *387*, 187−198.
(26) Pinto-Alphandary, H.; Balland, O.; Laurent, M.; Andremont, A.; Puisieux, F.; Couvreur, P. Intracellular Visualization of Ampicillin-Loaded Nanoparticles in Peritoneal Macrophages Infected in Vitro with *Salmonella typhimurium*. *Pharm. Res.* **1994**, *11*, 38−46.
(27) Forestier, F.; Gerrier, P.; Chaumard, C.; Quero, A. M.; Couvreur, P.; Labarre, C. Effect of Nanoparticle-Bound Ampicillin on the Survival of Listeria Monocytogenes in Mouse Peritoneal Macrophages. *J. Antimicrob. Chemother.* **1992**, *30*, 173−179.
(28) Sindhura Reddy, N.; Sowmya, S.; Bumgardner, J. D.; Chennazhi, K. P.; Biswas, R.; Jayakumar, R. Tetracycline Nanoparticles Loaded Calcium Sulfate Composite Beads for Periodontal Management. *Biochim. Biophys. Acta* **2014**, *1840*, 2080−2090.
(29) Li, L. L.; Xu, J. H.; Qi, G. B.; Zhao, X.; Yu, F.; Wang, H. Core-Shell Supramolecular Gelatin Nanoparticles for Adaptive and "On-Demand" Antibiotic Delivery. *ACS Nano* **2014**, *8*, 4975−4983.
(30) Becerril, H. A.; Mao, J.; Liu, Z.; Stoltenberg, R. M.; Bao, Z.; Chen, Y. Evaluation of Solution-Processed Reduced Graphene Oxide Films as Transparent Conductors. *ACS Nano* **2008**, *2*, 463−470.
(31) Stankovich, S.; Dikin, D. A.; Dommett, G. H.; Kohlhaas, K. M.; Zimney, E. J.; Stach, E. A.; Piner, R. D.; Nguyen, S. T.; Ruoff, R. S. Graphene-Based Composite Materials. *Nature* **2006**, *442*, 282−286.
(32) Wang, C. Y.; Li, D.; Too, C. O.; Wallace, G. G. Electrochemical Properties of Graphene Paper Electrodes Used in Lithium Batteries. *Chem. Mater.* **2009**, *21*, 2604−2606.
(33) Pasricha, R.; Gupta, S.; Srivastava, A. K. A Facile and Novel Synthesis of Ag−Graphene-Based Nanocomposites. *Small* **2009**, *5*, 2253−2259.
(34) Shi, Y.; Fang, W.; Zhang, K.; Zhang, W.; Li, L.-J. Photoelectrical Response in Single-Layer Graphene Transistors. *Small* **2009**, *5*, 2005−2011.
(35) Lv, X.; Huang, Y.; Liu, Z.; Tian, J.; Wang, Y.; Ma, Y.; Liang, J.; Fu, S.; Wan, X.; Chen, Y. Photoconductivity of Bulk-Film-Based Graphene Sheets. *Small* **2009**, *5*, 1682−1687.
(36) Sun, X.; Liu, Z.; Welsher, K.; Robinson, J. T.; Goodwin, A.; Zaric, S.; Dai, H. Nano-Graphene Oxide for Cellular Imaging and Drug Delivery. *Nano Res.* **2008**, *1*, 203−212.
(37) Liu, Z.; Robinson, J. T.; Sun, X.; Dai, H. PEGylated Nanographene Oxide for Delivery of Water-Insoluble Cancer Drugs. *J. Am. Chem. Soc.* **2008**, *130*, 10876−10877.
(38) Yang, X.; Zhang, X.; Liu, Z.; Ma, Y.; Huang, Y.; Chen, Y. High-Efficiency Loading and Controlled Release of Doxorubicin Hydrochloride on Graphene Oxide. *J. Phys. Chem. C* **2008**, *112*, 17554−17558.
(39) Misra, S. K.; Kondaiah, P.; Bhattacharya, S.; Rao, C. N. R. Graphene as a Nanocarrier for Tamoxifen Induces Apoptosis in Transformed Cancer Cell Lines of Different Origins. *Small* **2012**, *8*, 131−143.
(40) Zhang, L.; Xia, J.; Zhao, Q.; Liu, L.; Zhang, Z. Functional Graphene Oxide as a Nanocarrier for Controlled Loading and Targeted Delivery of Mixed Anticancer Drugs. *Small* **2010**, *6*, 537−544.
(41) Shimanovich, U.; Lipovsky, A.; Eliaz, D.; Zigdon, S.; Knowles, T. P.; Nitzan, Y.; Michaeli, S.; Gedanken, A. Tetracycline Nanoparticles as Antibacterial and Gene-Silencing Agents. *Adv. Healthcare Mater.* **2014**; DOI: 10.1002/adhm.201400631.
(42) Chattopadhyay, P.; Gupta, R. B. Production of Antibiotic Nanoparticles Using Supercritical CO_2 as Antisolvent with Enhanced Mass Transfer. *Ind. Eng. Chem. Res.* **2001**, *40*, 3530−3539.
(43) Zhang, J.; Yang, H.; Shen, G.; Cheng, P.; Zhang, J.; Guo, S. Reduction of Graphene Oxide via L-Ascorbic Acid. *Chem. Commun.* **2010**, *46*, 1112−1114.
(44) Sun, X.; Liu, Z.; Welsher, K.; Robinson, J. T.; Goodwin, A.; Zaric, S.; Dai, H. Nano-Graphene Oxide for Cellular Imaging and Drug Delivery. *Nano Res.* **2008**, *1*, 203−212.
(45) Ghadim, E. E.; Manouchehri, F.; Soleimani, G.; Hosseini, H.; Kimiagar, S.; Nafisi, S. Adsorption Properties of Tetracycline onto Graphene Oxide: Equilibrium, Kinetic and Thermodynamic Studies. *PLoS One* **2013**, *8*, No. e79254.
(46) Kiel, S.; Grinberg, O.; Perkas, N.; Charmet, J.; Kepner, H.; Gedanken, A. Forming Nanoparticles of Water-Soluble Ionic Molecules and Embedding them into Polymer and Glass Substrates. *Beilstein J. Nanotechnol.* **2012**, *3*, 267−276.
(47) Lellouche, J.; Kahana, E.; Elias, S.; Gedanken, A.; Banin, E. Antibiofilm Activity of Nanosized Magnesium Fluoride. *Biomaterials* **2009**, *30*, 5969−5978.
(48) Applerot, G.; Lellouche, J.; Perkas, N.; Nitzan, Y.; Gedanken, A.; Banin, E. ZnO Nanoparticle-Coated Surfaces Inhibit Bacterial Biofilm Formation and Increase Antibiotic Susceptibility. *RSC Adv.* **2012**, *2*, 2314−2321.
(49) Lellouche, J.; Friedman, A.; Lahmi, R.; Gedanken, A.; Banin, E. Antibiofilm Surface Functionalization of Catheters by Magnesium Fluoride Nanoparticles. *Int. J. Nanomed.* **2012**, *7*, 1175−1188.
(50) Malka, E.; Perelshtein, I.; Lipovsky, A.; Shalom, Y.; Naparstek, L.; Perkas, N.; Patick, T.; Lubart, R.; Nitzan, Y.; Banin, E.; Gedanken, A. Eradication of Multi-Drug Resistant Bacteria by a Novel Zn-Doped CuO Nanocomposite. *Small* **2013**, *9*, 4069−4076.
(51) Suslick, K. S. Sonochemistry. *Science* **1990**, *247*, 1439−1445.

DOI: 10.1021/acsami.5b00563
ACS Appl. Mater. Interfaces 2015, 7, 7324−7333

(52) Meridor, D.; Gedanken, A. Preparation of Enzyme Nanoparticles and Studying the Catalytic Activity of the Immobilized Nanoparticles on Polyethylene Films. *Ultrason. Sonochem.* **2013**, *20*, 425−431.
(53) Meridor, D.; Gedanken, A. Enhanced Activity of Immobilized Pepsin Nanoparticles Coated on Solid Substrates Compared to Free Pepsin. *Enzyme Microb. Technol.* **2014**, *67*, 67−76.
(54) Suslick, K. S.; Choe, S.-B.; Cichowlas, A. A.; Grinstaff, M. W. Sonochemical Synthesis of Amorphous Iron. *Nature* **1991**, *353*, 414−416.
(55) Gedanken, A. Doping Nanoparticles into Polymers and Ceramics Using Ultrasound Radiation. *Ultrason. Sonochem.* **2007**, *14*, 418−430.
(56) Krishnamoorthy, K.; Kim, G. S.; Kim, S. J. Graphene Nanosheets: Ultrasound Assisted Synthesis and Characterization. *Ultrason. Sonochem.* **2013**, *20*, 644−649.
(57) Gamliel, H. Optimum Fixation Conditions May Allow Air Drying of Soft Biological Specimens with Minimum Cell Shrinkage and Maximum Preservation of Surface Features. *Scanning Electron Microsc.* **1985**, 1649−1664.
(58) Park, S.; Ruoff, R. S. Chemical Methods for the Production of Graphenes. *Nat. Nanotechnol.* **2009**, *4*, 217−224.
(59) Compton, O. C.; Nguyen, S. T. Graphene Oxide, Highly Reduced Graphene Oxide, and Graphene: Versatile Building Blocks for Carbon-Based Materials. *Small* **2010**, *6*, 711−723.
(60) Chen, R. J.; Zhang, Y.; Wang, D.; Dai, H. Noncovalent Sidewall Functionalization of Single-Walled Carbon Nanotubes for Protein Immobilization. *J. Am. Chem. Soc.* **2001**, *123*, 3838−3839.
(61) Liu, Z.; Sun, X.; Nakayama-Ratchford, N.; Dai, H. Supramolecular Chemistry on Water-Soluble Carbon Nanotubes for Drug Loading and Delivery. *ACS Nano* **2007**, *1*, 50−56.
(62) Mattevi, C.; Eda, G.; Agnoli, S.; Miller, S.; Mkhoyan, K. A.; Celik, O.; Mastrogiovanni, D.; Granozzi, G.; Garfunkel, E.; Chhowalla, M. Evolution of Electrical, Chemical, and Structural Properties of Transparent and Conducting Chemically Derived Graphene Thin Films. *Adv. Funct. Mater.* **2009**, *19*, 2577−2583.
(63) Nikaido, H. Multidrug Resistance in Bacteria. *Annu. Rev. Biochem.* **2009**, *78*, 119−146.
(64) Shaobin, L.; Tingying Helen, Z.; Mario, H.; Ehdi, B.; Jun, W.; Rongrong, J.; Jing, K.; Yuan, C. Antibacterial Activity of Graphite, Graphite Oxide, Graphene Oxide, and Reduced Graphene Oxide: Membrane and Oxidative Stress. *ACS Nano* **2011**, *9*, 6971−6980.

DOI: 10.1021/acsami.5b00563
ACS Appl. Mater. Interfaces 2015, 7, 7324−7333